SANDIA REPORT

SAND 2004-5253
Unlimited Release
Printed November 2004

Equation of state and electrical conductivity of stainless steel

Thomas R. Mattsson
Michael P. Desjarlais

Prepared by
Sandia National Laboratories
Albuquerque, New Mexico 87185 and Livermore, California 94550

Sandia is a multiprogram laboratory operated by Sandia Corporation,
a Lockheed Martin Company, for the United States Department of Energy's
National Nuclear Security Administration under Contract DE-AC04-94AL85000.

Issued by Sandia National Laboratories, operated for the United States Department of Energy by Sandia Corporation.

Available to DOE and DOE contractors from
U.S. Department of Energy
Office of Scientific and Technical Information
P.O. Box 62
Oak Ridge, TN 37831

Telephone: (865)576-8401
Facsimile: (865)576-5728
E-Mail: reports@adonis.osti.gov
Online ordering: http://www.osti.gov/bridge

Available to the public from
U.S. Department of Commerce
National Technical Information Service
5285 Port Royal Rd
Springfield, VA 22161

Telephone: (800)553-6847
Facsimile: (703)605-6900
E-Mail: orders@ntis.fedworld.gov
Online order: http://www.ntis.gov/help/ordermethods.asp?loc=7-4-0#online

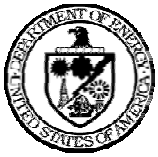

SAND 2004-5253
Unlimited Release
Printed November, 2004

Equation of state and electrical conductivity of stainless steel

Thomas R. Mattsson
Michael P. Desjarlais
HEDP Theory and ICF Target Design, org. 1674
Sandia National Laboratories
P.O. box 5800
Albuquerque, NM 87185-1186

Abstract

Warm dense matter is the region in phase space of density and temperature where the thermal, Fermi, and Coulomb energies are approximately equal. The lack of a dominating scale and physical behavior makes it challenging to model the physics to high fidelity. For Sandia, a fundamental understanding of the region is of importance because of the needs of our experimental HEDP programs for high fidelity descriptive and predictive modeling. We show that multi-scale simulations of macroscopic physical phenomena now have predictive capability also for difficult but ubiquitous materials such as stainless steel, a transition metal alloy.

Acknowledgements

Tom Mehlhorn is acknowledged for valuable discussions as well as for managing the project. We wish to thank Kyle Cochrane for formatting the EOS and conductivity tables for use in ALEGRA as well as testing the tables and doing simulations. Stephen Rosenthal is acknowledged for performing the exploding wire simulations and analyzing the results. Jeremy Johnson is acknowledged for running some of the QMD simulations.

The simulations were run at C-plant (New Mexico), Sandia's QT cluster (New Mexico), as well as on the Pulsed Power Sciences Center's cluster koopa.

Table of contents

List of Figures

Equation of state and electrical conductivity of stainless steel

1. About the project

This SAND report is the final report of the LDRD project "Electrical conductivity of metal alloys". The scientific work has during the course of the project been presented at a number of international conferences, including the Division of Plasma Physics (DPP) meeting in Albuquerque (2003), the March meeting of the American Physical Society in Montreal (2004), and the14th APS topical conference on Atomic Processes in Plasmas in Santa Fe (2004). Mike Desjarlais has been invited to the DPP meeting in Savannah, Georgia this fall to present this work.

The report is organized as follows: The first section is a general introduction as well as a summary of the most important findings; subsequent sections present technical details documenting the process of developing a wide-range equation of state model including electrical conductivity.

2. Introduction and highlights of results

Traditionally topics of astrophysics, shock-physics, and fusion; a wide range of high-energy density physics (HEDP) phenomena are currently studied in controlled laboratory conditions using sophisticated drivers like high-powered lasers or Z-pinches [1]. Laboratory experiments have already revealed details of physical phenomena otherwise difficult to explore. The new generation of facilities scheduled to be operational in the near future, like the National Ignition Facility (NIF) and the refurnished Z machine (Z/R), will significantly extend the range of conditions of matter possible to study. Although experimental capabilities are the main focus of the efforts, numerical simulations constitute integral parts of contemporary experimental development; simulations are employed to design experiments years ahead of their realization [2,3] as well as frequently after experiments to assess the outcome and compare to predictions.

High-fidelity simulations of HEDP systems are demanding since many physical processes contribute critically to the design of experiments, for example it was very recently demonstrated that pre-heating effects could have a profound impact on the yield at NIF [4]. Macroscopic rad-hydro simulation codes (ALEGRA, LASNEX) are utilized to predict and post-analyze experiments. Since the thermodynamic evolution of a system is determined by the detailed properties of the materials, the simulations require physics models for various materials: aluminum, beryllium, copper, steel, gold, etc. Equations of state (EOS) and electrical conductivities are two key properties required to high accuracy over a wide range of phase-space for the simulations to be predictive.

The area in phase-space where the thermal-, Fermi-, and Coulomb energies are approximately equal: $k_BT \sim E_F \sim E_e$ is often denoted the warm-dense matter (WDM) regime (see Fig. 1). The WDM region is central to many HEDP experiments since it is either traversed (laser drive) or the region where important dynamics such as the metal insulator transition take place (Z-pinch drive). Somewhat surprisingly, properties like the electrical conductivity were recently not modeled to sufficiently high accuracy to allow for predictive simulations despite the complexity of today's rad-hydro simulation codes. For example, the physics of Al flyer plate experiments probing the Hugoniot of deuterium [5] could not be simulated with rad-hydro methods before QMD simulations [6] improved the understanding and yielded quantitative results [7]. When Al, a simple metal with few electrons and no d-shell, turns out to be too demanding for traditional methods, there is reason to take a closer look at how to model more complex materials in the WDM regime.

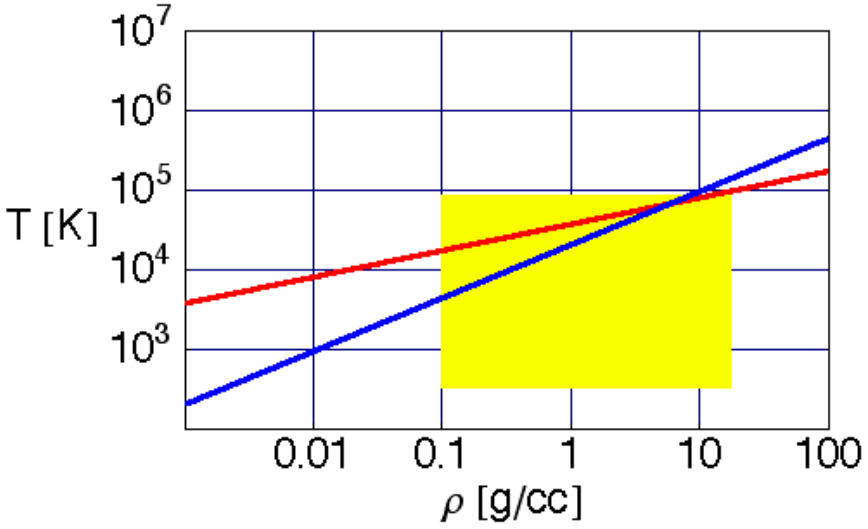

Figure 1. Phase space of density and temperature with the Fermi energy (blue) and Coulomb energy (red) for Iron. QMD simulations are routinely performed in the yellow area spanning 2-3 orders of magnitude in density (10^{-2} to 15 g/cc) and temperatures from 0K to 9 x10^4 K. Hence, the WDM region is described from a quantum mechanical viewpoint without additional assumptions regarding dominating physical mechanisms. At higher and lower densities, as well as higher temperatures, standard models are often sufficient.

With incomplete physics models even otherwise sophisticated macroscopic simulations fail, resulting in a detailed study of a faulty materials model -- not the real system. Fig. 1 illustrates the difficulties inherent in modeling WDM. It is the region where high-temperature plasma physics meets low-temperature condensed matter physics. High-fidelity simulations require physics models that are based on reliable information directly from this regime and not extrapolated from low- or high-temperatures. In addition, direct experimental data is rarely available in this regime; results from experiments are extracted from post-experiment analysis including modeling of, for example, the energy balance in the experiment.

In this article we present theoretical results for stainless steel in the WDM regime. Steel is the material of transmission lines on Z as well as suggested as a material for wires on Z/R. Steel is modeled as an alloy of Fe, Cr, and Ni; all three elements are computationally demanding and the presented progress in modeling steel infers that many metals can be approached using the same methodology.

2.1. Method

The HEDP systems primarily in focus of this work, Inertial Confinement Fusion (ICF), and materials experiments with flyer plates, exhibit physics on several scales: the equation of state and electrical conductivity is determined on the atomistic scale where quantum mechanics governs the behavior; wires and flyer-plates are of dimensions μm to mm and radiation-magneto-hydrodynamic simulations (Rad MHD) are the appropriate computational approach; transmission lines and capacitors are on the scale of meters and modeled as circuit elements. Predictive modeling requires integration of all scales, including the atomistic; the flyer-plate experiments [7] described above became predictive as a direct consequence of the quantum mechanical simulations of atomic properties.

We employ Density Functional Theory (DFT) [9] for a first-principles analysis of the electronic structure. DFT is formally exact with the exchange-correlation (XC) functional as its only approximation. The generalized gradient approximation (GGA) [10] is regarded as the functional of choice for Fe and is used throughout. The simulations were made with VASP [11] using PAW pseudo-potentials [12]. A plane-wave cutoff energy of 500 eV was determined by convergence of the pressure; the cutoff required is significantly higher than what is necessary for more traditional DFT calculations of energy difference

between structures. The calculations are, after choice of XC-functional, without free parameters. The electronic structure, with its resulting interaction between ions, is fully governed by quantum mechanics.

By sampling the pressure in molecular dynamics (MD) simulations in the NVT ensemble the equation of state P(ρ,T) is calculated. The MD simulations are between 2-5 ps long, depending on thermalization times, for each point in phase-space. Phase transitions--- liquid-solid, liquid-vapor, vapor-liquid --- have been observed when changes in (ρ,T) move the system across a phase-boundary. However, because of the small size of the simulated system, there is considerable hysteresis in these phase changes.

From the equilibrium time-span of the calculation we extract a number of configurations for which the frequency dependent electrical conductivity is calculated using the Kubo-Greenwood formalism [6]. The DC electrical conductivity is calculated as lim ω -> 0 of σ(ω). The frequency dependent opacities for low to moderate photon energies are also calculated using the Kramers-Krönig relations.

The approach presented above yields fundamentally consistent EOS, conductivity and opacity information for a material. The consistency is of key importance, in particular in the WDM regime, where extrapolation of models generated within different frameworks and regions of validity is the more common approach.

2.2. Equation of State of stainless steel

The QMD steel EOS in the WDM region is shown in Fig. 2. The liquid-vapor critical point of steel is calculated to be 10 000 K at 2 g/cc and a pressure of 6 kbar. Compared to the most recent SESAME [13] table for stainless steel, 4272, the critical point is moved 2000 K higher in this work; a change that is likely to affect rad-hydro simulations in the WDM region.

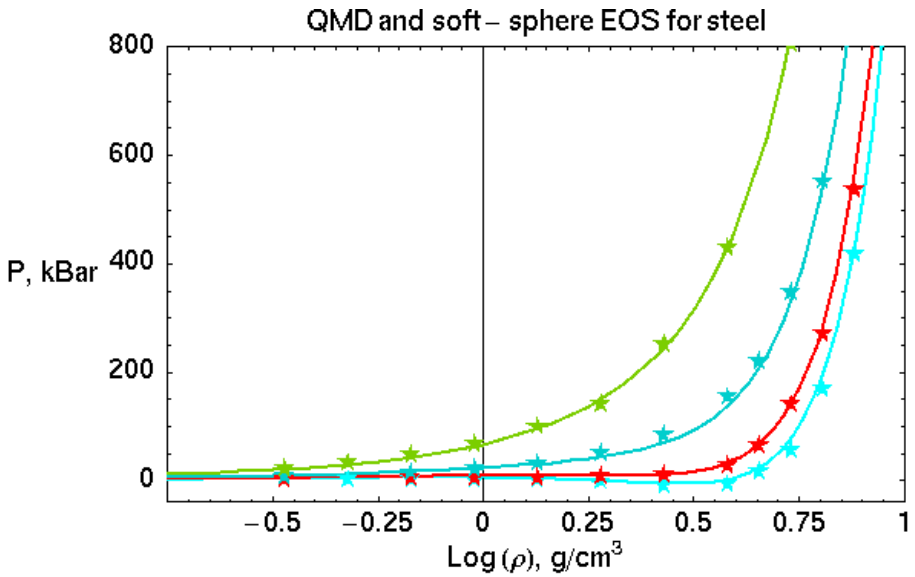

Figure 2. Equation of state for steel in the WDM regime. Temperatures shown are 8, 10, 16, and 30 kK for QMD (symbols) and the fitted soft-sphere model (lines).

In order to interpolate between the QMD data points in a thermodynamically consistent manner we mapped the QMD results onto a thermodynamically consistent model EOS, the soft-sphere model [13], the fitted SS model is subsequently used to calculate the EOS on a dense enough grid for use in rad-hydro codes. The soft-sphere fits are also shown in Fig. 2. A standard soft-sphere model with fixed parameters will not fit the pressures over more than a narrow interval in temperature: only by allowing for temperature-dependent parameters was it possible to fit a wide-range of temperatures. The use of temperature dependent parameters makes it necessary to explicitly calculate the internal energy using the

thermodynamic identity instead of the standard expressions for internal energy in the soft-sphere model. The soft-sphere model is smoothly merged with the 4272 SESAME table and changes the properties in the region 4000 < T < 50 000 K, outside this region we employ the table as is. The final result is a tabulated thermodynamically consistent table for steel that is now available for use in rad-hydro simulations.
The largest differences with the SESAME 4272 table are found in the region surrounding the critical point, as shown in Fig. 3.

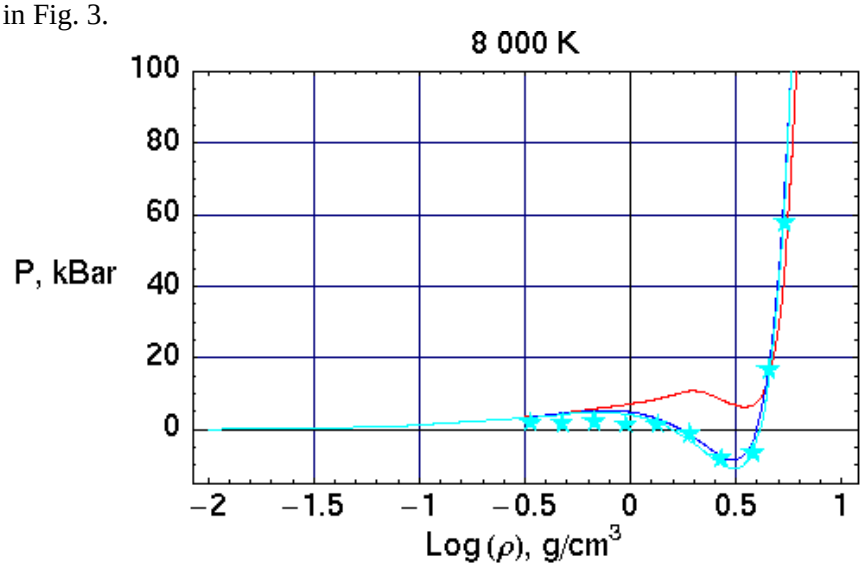

3. Pressure as a function of density at 8000 K: QMD (symbols), Soft-Sphere best fit (Turquoise), soft-sphere parameterized model (blue), and SESAME 4272 (red).

2.3. Electrical conductivity of stainless steel

The thermo-physical property with the most important changes from the QMD calculations is the electrical conductivity. The approach to low-density is particularly sensitive to quantum localization; the free-electron like behavior of a dense metal gradually changes to the insulating behavior of neutral atoms at low density. In addition, ionization must be modeled to correctly capture the high temperature behavior. These mechanisms are implicitly included in the QMD/ Kubo-Greenwood modeling at an *ab initio* level, without additional assumptions or constraints, making the current approach very suitable to the WDM regime.

Fig. 4 shows the electrical conductivity of stainless steel as a function of density and temperature. The rapid decrease in conductivity with lowering density at lower temperatures is a result of the localization of electrons on ions in the absence of significant thermal ionization. At higher temperatures and lower densities, thermal ionization aided by an increasing density of states, maintains higher conductivities. Previous conductivity models, such as the Lee-More and Rinker SESAME models, are orders of magnitude in error in this regime [8]. The LM model uses a Thomas-Fermi model for the electrons and thus does not include orbital effects and the Rinker model (based on Ziman's theory) is strictly not valid, although sometimes extrapolated into the WDM regime.

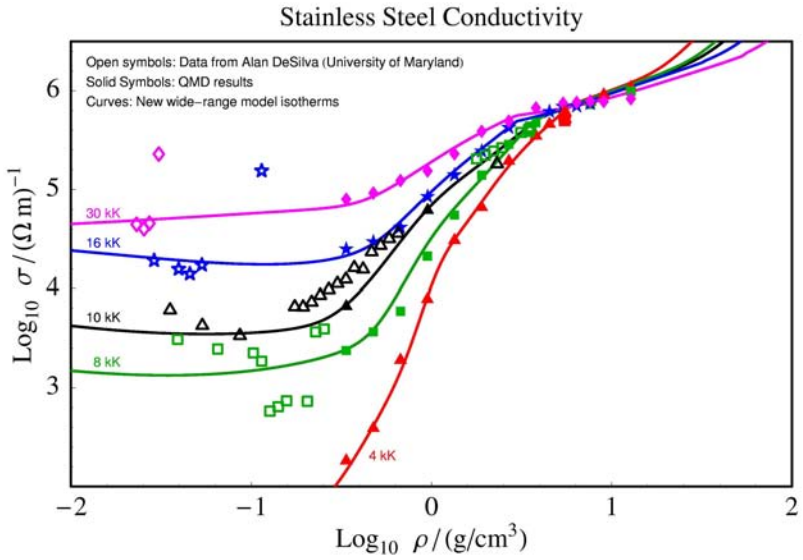

Figure 4. Electrical conductivity for stainless steel: QMD results (symbols), wide-range model based on QMD (lines) and experimental results (open symbols).

2.4. Simulation of an exploding steel wire

Predictive simulations of a wire explosion are the basis for being able to do predictive calculations of full wire-array implosions of a Z-pinch. It is a challenging problem since the rapid current flow through the wire involves modeling the wire from solid state to dense plasma in a time span of a few ns. Initially, the current flows through the solid wire, which is rapidly heated. As matter is evaporated from the wire, forming a gas outside the wire, current begins going flowing through this material, heating it, and generating a coronal plasma, the formation of which depends crucially on the conductivity and EOS. Previous conductivity models for steel did not display the correct physics, even qualitatively. Replacing the old models with a QMD derived conductivity model turned largely meaningless modeling into quantitative, predictive simulations, as shown in Fig. 4.

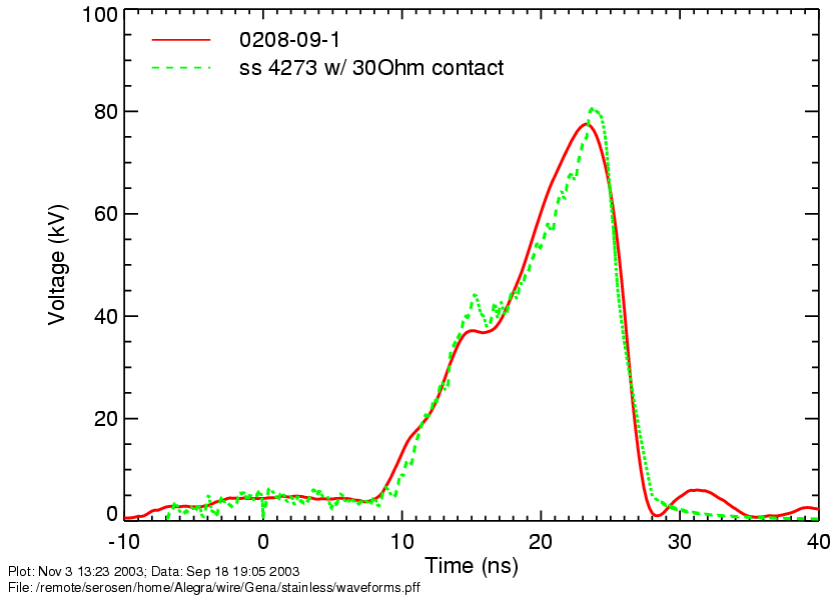

Figure 5. Voltage pulse from experiments and simulations, the breakdown is reproduced with ns accuracy and important features of the pulse shape are correctly described. The behavior after breakdown (28 ns) is not significant.

2.5. Summary and conclusions

Progress in the field of computer simulations of HEDP system is made in several areas. There is ongoing development of rad-hydro simulations by increasing the efficiency, precision and capabilities. In addition to this important work, we argue on the basis of our experience in utilizing and exploring previously considered state-of-the-art physics models for several materials that a most important area of research is to develop high-fidelity materials models. Not only are accurate materials models important for doing predictive simulations today, they are also important for the future development of macroscopic HEDP simulation methods since remaining discrepancies more easily can be attributed to deficiencies in algorithms and approximations if the underlying physics model is trusted. First-principle based simulations of HEPD materials have the potential to become increasingly important in the future as the expectations of simulations are raised.

3. QMD simulations of HEDP systems

Density Functional Theory (DFT) [9] is the method of choice for large-scale quantum simulations and has been employed in materials science, condensed matter physics, physical chemistry, and chemistry for decades. In the last few years DFT has been increasingly applied to HEDP systems, with good results. The only approximation, besides numerical precision in calculations, is the choice of exchange-correlation functional. For Fe, it is common knowledge that the GGA [10] is the most suitable functional and we use it throughout for the simulations.

3.1. Convergence

A crucial part of a DFT calculation is to establish convergence. Calculating thermodynamic properties, like pressure, in the HEDP regime requires the same type of convergence tests as more standard, low temperature simulations; however, the final demands are different. The most notable exception to normal-low temperature calculations is the high cutoff energy necessary for an accurate description of the electronic pressure. Regarding k-point sampling, two factors reduce the number of k-points required: first, the thermal disorder of the ions is significant, there is no periodicity except for the supercell itself; second, the high electronic temperature, 0.5 to 8 eV, has a smoothing effect on the band structure, requiring less extensive k-point sampling, using only the gamma-point is sufficient in most cases.

3.1.1. Spin

Electronic spin is of highest importance in determining thermo-physical properties of Fe at low temperatures. The warm-dense-matter regime --- a region of the phase-diagram of great interest to Sandia's HEDP research --- is well above the Fe Curie temperature (T_C=1043 K). Thus there exists no *global* spin order in this regime, and the lack of order increases for higher temperature. We have studied at which temperature it becomes necessary to include spin by investigating a small model system at different temperatures. The results are shown in Fig. 6.

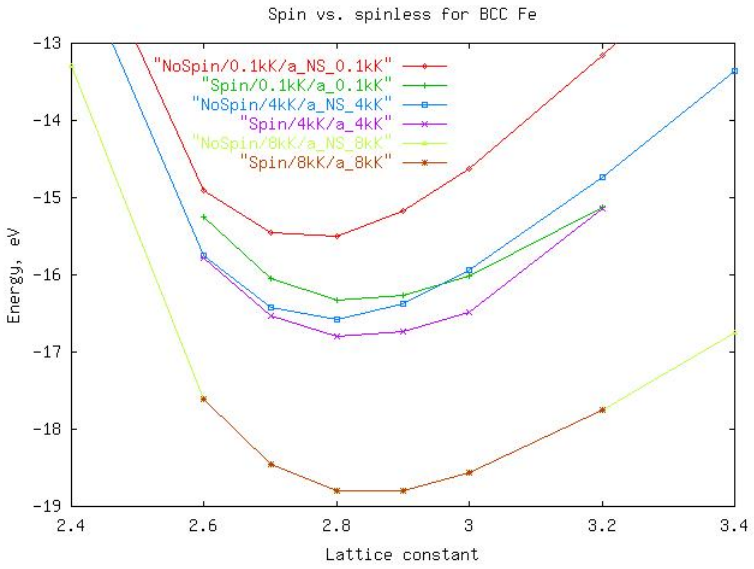

Figure 6. The effect of spin on BCC iron; for temperatures above 8000 K spin has effect on neither the energy nor the resulting lattice constant.

Since the effects of spin are undetectable above 8000 K, the region of which we are most interested in, neglecting spin is an acceptable approximation.

3.2. QMD EOS

During the molecular dynamics simulations the system evolves through different configurations and once equilibrium has been reached the pressure, energy, and other state-variables can be sampled. The state-variables are calculated as running averages with variable initial/final sampling times, the final value is taken as an average over the running average, minimizing statistical fluctuations. The resolution in temperature is high, as shown in Fig. 7. Two isotherms from runs at 10 000 K and 10 500 K are clearly resolved, resulting in the expected change in pressure. The statistical errors are evidently small, verifying that our sampling methodology is adequate.

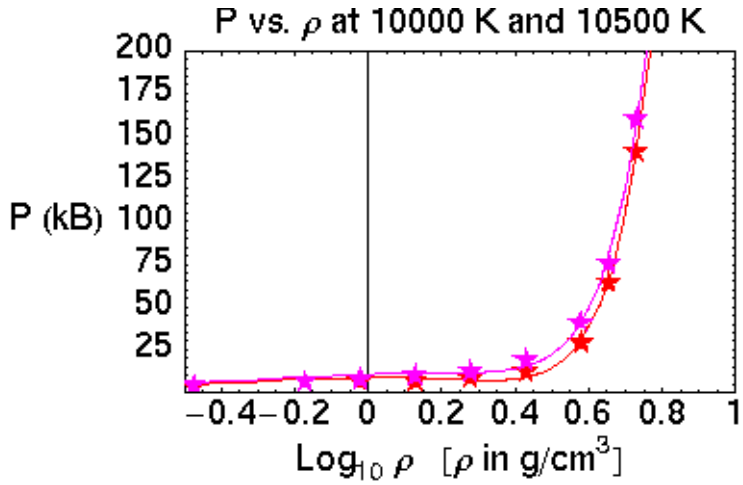

Figure 7. QMD pressures for 10 000 K (red symbols) and 10 500 K (pink symbols) with the corresponding optimal soft-sphere model fits shown. The statistical sampling is adequate to distinguish between two states only 5% apart in temperature.

4. Equation of State

The range of EOS for use in for Sandia important applications is very large, exploding wires and flyer plates start as cold solid metal and within a few ns their state has evolved into a hot plasma with temperatures reaching several eV. The QMD EOS can be calculated for a limited number of points of phase-space, although we have done more than one hundred points the macroscopic simulations require a denser grid. Two questions must be addressed: how to interpolate between QMD points and how to extrapolate to regions not accessible to QMD.

4.1. Soft-sphere model

The soft-sphere model [14] has been applied to liquid metals for a number of years [15,16]; it includes a liquid-vapor phase-transition with a critical point. The model is based on Monte-Carlo simulations of soft spheres [17]. The model has a few parameters modifying the ideal-gas equation of state, yielding a critical point and phase transition. The low-density regime and the soft-sphere energy as a function of density for high temperature were not possible to fit without adding a thermal ionization term in the soft-sphere model.

$$P(\rho,T) = P_{ideal}(\rho,T) \times \left[1 + Z(T) + \frac{1}{3} n C_n \rho^{n/3} \left(\frac{\varepsilon}{kT} \right) + \frac{1}{18} n(n+4) \rho^{n/9} \left(\frac{\varepsilon}{kT} \right)^{1/3} - \rho^m \left(\frac{\varepsilon}{kT} \right) \right]$$

Eq. 1

The thermal ionization Z(T) is a monotonic function of temperature and is shown in Fig. 8. It was chosen to fit the energy at high temperature as well as the pressure at low density and making the parameters n, ε, and m smooth functions of temperature: n(T), ε(T), and m(T). The pressure expression is hence a more complex function of temperature than the original soft-sphere expression.

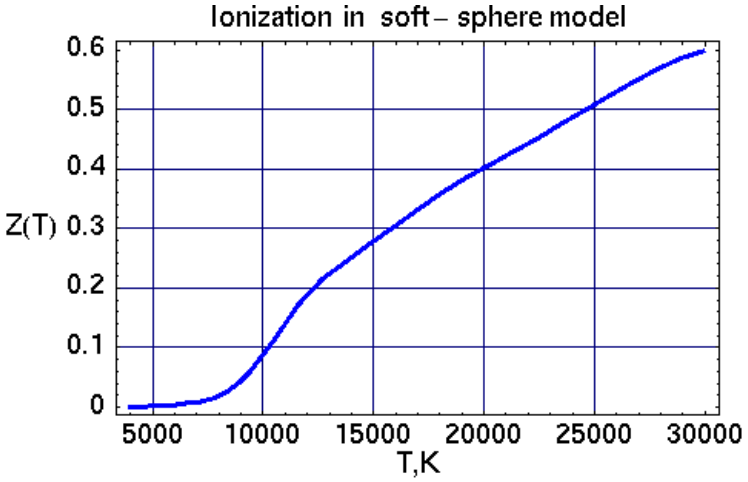

Figure 8. Thermal ionization Z(T) in the modified soft-sphere model of Eq. 1.

4.2. Fitting to QMD data

A single parameter fit does not satisfactorily describe steel even across the range of phase-space covered by the QMD simulations; we are therefore required to extend the soft-sphere model to increase the region of acceptable fit to the QMD results.

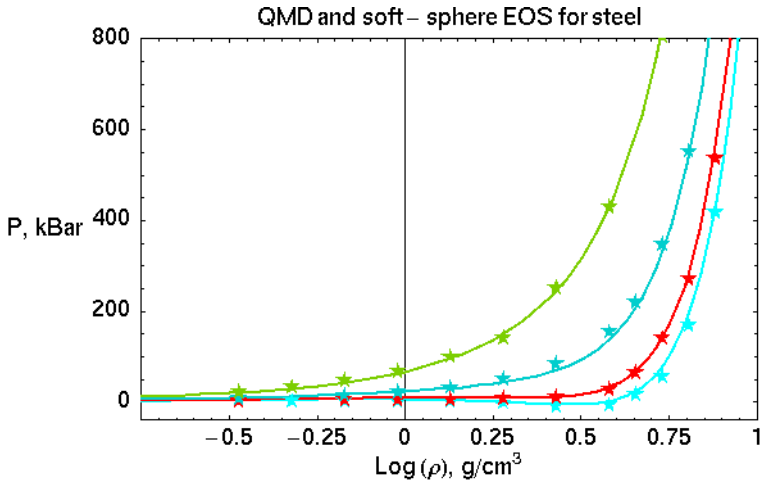

Figure 9 Soft-sphere model fits of pressure with temperature-dependent parameters. QMD results (symbols) for 8, 10, 16, and 30 kK. The model captures the main QMD behavior.

The model parameters were allowed to depend monotonically on temperature, as shown in Fig. 7. The special character of the critical point shows up in the parameterizations as well as in the pressure itself.

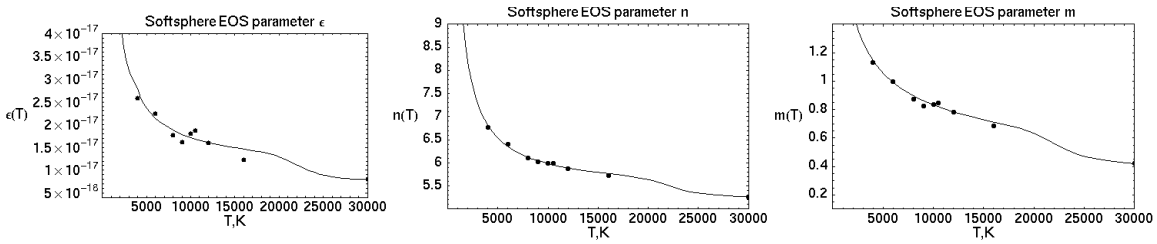

Figure 10. Temperature dependences of three soft-sphere model parameters: ε, n, and m, which are allowed to be functions of temperature. The points correspond to the optimal parameters at each temperature; these best-fit parameters are employed in Figs 7 and 9.

We chose pressure instead of energy as primary in the fit because of the more distinct features in pressure surrounding the critical point; Fig. 11 shows the pressure and energy surrounding the critical point. The energy changes slowly with no qualitative change in behavior as well as with larger spread in the data points. The pressure, on the other hand, exhibits a loss in negative curvature pinpointing the critical point. The fits were made solely on pressure but the energy is represented well using the same parameters. The opposite procedure, however, fitting with respect to energy and comparing with pressure does not work as well (not shown) due to the slow qualitative changes in energy behavior.

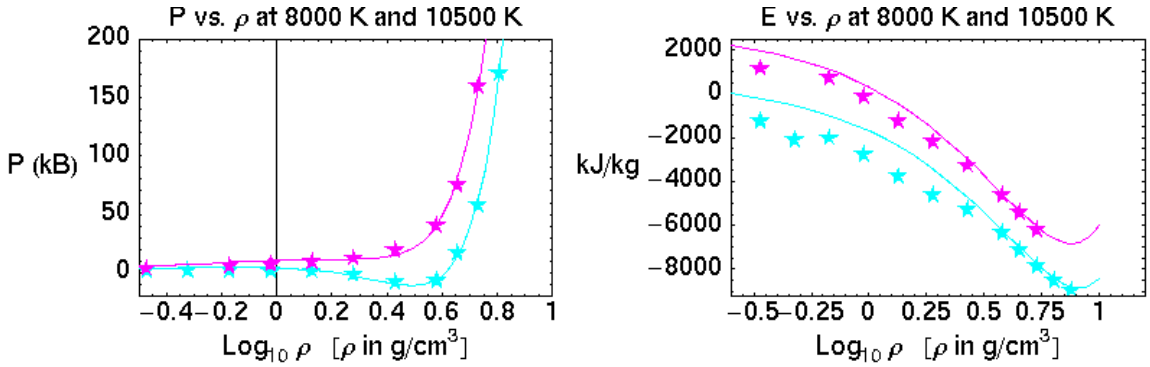

Figure 11. The behavior for steel above (10500 K) and below (8000 K) the critical point for pressure (left) and energy (right). QMD results (symbols) and pressure soft-sphere fits

(lines). The behavior is significantly more pronounced in pressure than in energy; the pressure is therefore used to fit the model.

The interpolation properties of our approach seems excellent, as illustrated in Fig. 12, where the soft-sphere model pressure for 22 000 K is shown, as calculated *before* performing the QMD simulations at the same temperature. The model EOS was based on fits at 16 000 K and 30 000 K in addition to several temperatures in, and below, the critical region, all QMD points used in fitting are shown in Fig. 10.

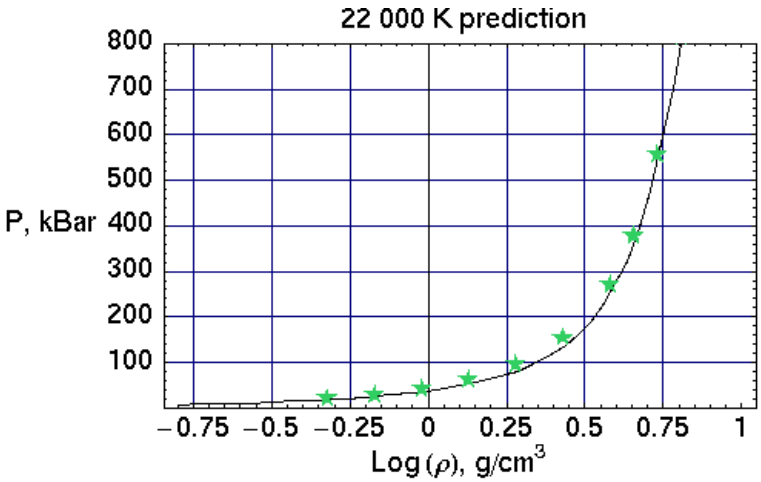

Figure 12. Prediction of pressure at 22 kK using the model (black line); QMD *post facto* calculation (symbols). The model interpolates well in the WDM regime.

The intricate temperature dependencies of the soft-sphere model with T-dependent parameters required us to enforce thermodynamic consistency explicitly by thermodynamic integration of the pressure

$$\rho^2\left(\frac{\partial E}{\partial \rho}\right) = P - T\left(\frac{\partial P}{\partial T}\right)$$

$$dE = \frac{1}{\rho^2}\left(P - T\frac{dP}{dT}\right)d\rho$$

Eq. 2

Integrating Eq. 2 yields an expression for the energy.

$$E_2 = E_1 + \int_1^2 \frac{1}{\rho^2}\left(P - T\frac{dP}{dT}\right)d\rho.$$

Eq. 3

The approach has a significant advantage in being manifestly thermodynamically consistent; a superficial limitation is that the energy cannot be written in closed form as in the original soft-sphere model but since SESAME format tables are generated in the end, this is of little consequence.

4.3. Merging with SESAME 4272

Outside the QMD range we merge the soft-sphere model with a recent SESAME table for stainless steel, 4272. As the model was fitted against the QMD pressure we merge pressures as

$$P(\rho,T) = \alpha(\rho)\beta(T)P_{SS}(\rho,T) + \left[1-\alpha(\rho)\beta(T)\right]P_{4272}(\rho,T).$$

Eq. 4

Where α(p) and β(T) are smooth blending functions in temperature and density, shown in Fig. 13. The energy is subsequently calculated using Eq. 3 for the combined model. Merging the two methods required

tuning by hand, the additional temperature dependence of the merging function can cause crossing isotherms in pressure and/or energy if not carefully selected. Since the blending is sensitive to details in the blending functions it is likely that the blending can be improved further, but the currently implemented functions are conservative and yields separated isotherms.

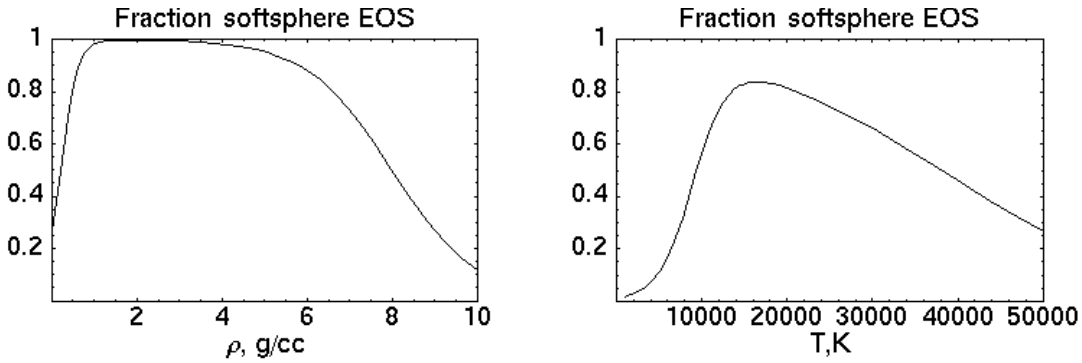

Figure 13. Blending functions α(ρ) (left) and β(T) (right) merging the soft-sphere pressure with SESAME 4272 creating a wide-range model modified in the WDM regime.

The resulting EOS has been implemented in the SESAME format; it is available for use in ALEGRA and currently employed in wire simulations. Fig. 14 shows three isotherms of the implemented table, there are no crossing isotherms and the model smoothly extends into the SESAME 4272 table at high and low density, as well as for high and low temperature.

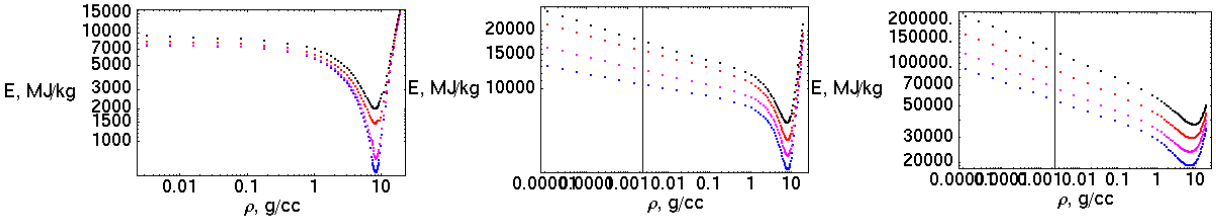

Figure 14. Energy isotherms for the implemented model at three sets of four temperatures below, at and above T_c: 1500, 1900, 3010, and 4266 K (left); 8128, 9550, 11220, and 13183 K (center); 29.5, 34.7, 40.7, and 47.9 kK (right). The table's temperature grid is exponential.

5. Electrical conductivity

The electrical conductivity is arguably the most important progress in describing the physical properties of metals gained from the QMD simulations. The behavior of Al flyer plates could not be simulated until modified conductivity models were employed [6,7,8]. The methodology has been described elsewhere [6,7,8], here we present a brief summary of the process and present the results for stainless steel.

From the equilibrated segment of the MD simulation of the order 10-20 configurations are extracted at equal intervals and subjected to a Kubo-Greenwood transport calculation [6,7,8]. The frequency dependent conductivity, σ(ω), is calculated for each configuration and averaged over all extracted as well as over the three spatial directions to form the conductivity at that point in phase-space. The DC-conductivity is obtained as the zero frequency limit of σ(ω). The conductivities for single geometries vary but when averaged over 10-20 configurations a well-defined behavior emerges, as shown in Fig. 15. The dip at very low energies is not physical and results from the discrete nature of the eigenvalue spectrum inherent in a finite simulation.

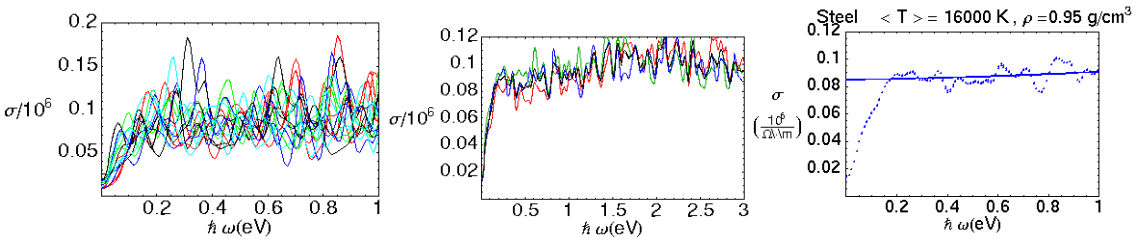

Figure 15. Calculating the electrical conductivity. σ(ω) for 15 geometries (left); . . averaged in the x, y, and z directions(center); Extrapolation to zero frequency (right). The case shown is for 16 kK and ρ = 0.95 g/cc. Averaging is key to a reliable conductivity.

The resulting QMD/ Kubo-Greenwood conductivities are shown in Fig. 13, together with the wide-range model developed within the project. The new wide-range model of the electrical conductivity was generated using Desjarlais' [8] extension of the Lee-More model, often referred to in the literature as the Lee-More-Desjarlais (LMD) model. The complexity of the parameterization with the LMD framework precluded an algorithmic model for stainless steel and only a SESAME format table was generated.

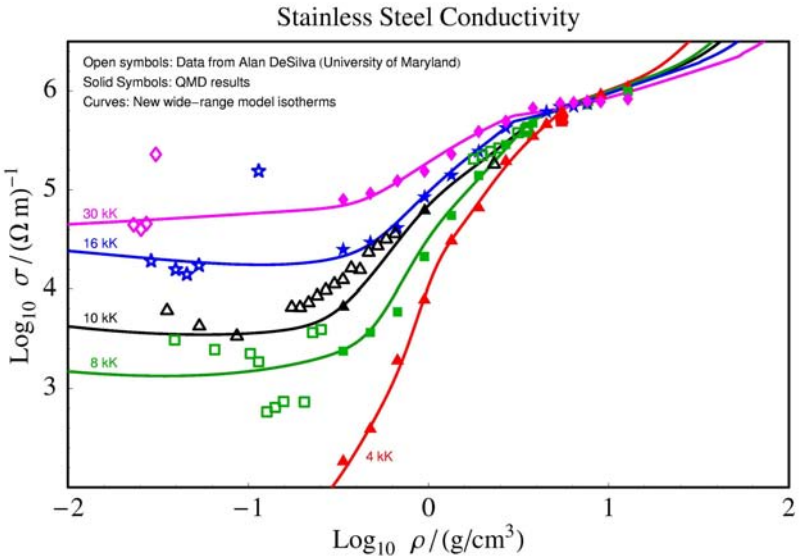

Figure 16. Electrical conductivity of stainless as a function of temperature and density.

As a part of the LDRD project we funded professor DeSilva at University of Maryland to carry out exploding wire simulations for measuring the conductivity of steel wires. The results are shown in Fig. 16 together with the QMD results and the wide-range model. Note that the experiments themselves are subject to inaccuracies and scatter among points. In particular, the temperature is inferred through an assumed EOS for the stainless steel, an approach that can easily give 10 to 15% uncertainty in the temperature. Within the experimental uncertainty, the experiments support the QMD calculations.

The wide-range conductivity model has been used in exploding wire simulations and the results presented in Fig. 5. We obtain quantitative agreement between theory and simulations; the voltage collapse is reproduced to ns accuracy.

6. Summary

With macroscopic rad-hydro simulations becoming increasingly capable of describing the physics of HEDP systems and first-principles methods becoming relevant to the HEDP regime there has been renewed interest in the development of fundamental physics models. The project has shown that DFT

based modeling of key physical properties is possible also for highly demanding systems, like stainless steel. The conductivity model developed as a part of this project has a profound impact on the quality of the macroscopic rad-hydro simulations of exploding steel wires; the QMD-EOS results confirm that SESAME 4272 is an adequate EOS for steel in describing exploding wires and also gives us confidence that our QMD methods may be used to generate a high quality EOS where no other alternative is available.
The project has resulted in a unique expertise being created at Sandia regarding first-principles modeling of HEDP systems in general and the integration of QMD results into rad-hydro codes in particular.

Not only are accurate materials models important for doing predictive simulations today, they are also important for the future development of macroscopic HEDP simulation methods since remaining discrepancies between experiments and simulations more easily can be attributed to deficiencies in algorithms and approximations if the underlying physics models are trusted.

The project has, in our view, shown that first-principle based simulations of HEPD materials have the potential to become increasingly important in the future as the expectations of the performance of simulations are raised.

References

[1] Frontiers in High Energy Density Physics: The X-games of contemporary science, National Research Council of the National Academies, (2003).
[2] J.A. Paisner, E.M. Campbell, and W.J. Hogan, Fusion Technology **26**, 755 (1994).
[3] L. Suter, J. Rothenberg, D. Munro, B. van Wonterghem, and S. Haan, Physics of Plasmas, **7**, 2092 (2000).
[4] R.E Olson, R.J. Leeper, A. Nobile, and J.A. Oertel, Physical Review Letters **91**, 235002 (2003).
[5] M.D. Knudson, D.L. Hanson, J.E. Bailey, C.A. Hall, J.R. Asay, and W.W. Anderson, Physical Review Letters **87**, 225501 (2001).
[6] M.P. Desjarlais, J.D. Kress, and L.A. Collins, Physical Review E **66**, 025401 (2002).
[7] R.W. Lemke, M.D. Knudson, C.A Hall, T.A. Haill, M.P. Desjarlais, J.R. Asay, and T.A. Mehlhorn, Physics of Plasmas **10**, 1092 (2003).
[8] M. P. Desjarlais, Contrib. Plasma Phys. **41**, 267 (2001).
[9] P. Hohenberg and W. Kohn, Physical Review **136**, B864 (1964); W. Kohn and L. Sham, Physical Review **140**, A1133 (1965).
[10] J.P. Perdew et al. Physical Review B **46**, 1253 (1992); Physical Review E **40**, 4978 (1993).
[11] G. Kresse and J. Hafner, Physical Review B **47**, 558 (1993); G. Kresse and J. Hafner, Physical Review B **49**, 14251 (1994); G. Kresse and J. Furthmuller, Physical Review B **54**, 11169 (1996);
[12] P.E. Blochl, Physical Review B **50**, 17953 (1994); G. Kresse and D. Joubert, Physical Review B **59**, 1758 (1999).
[13] SESAME, Equation of State Tables, Los Alamos.
[14] D.A. Young, "A soft-sphere model for liquid metals", LLNL (1977).
[15] G.R Rathers, J.W. Shaner, and D.A. Young, Physical Review Letters **33**, 70 (1974).
[16] F. Hensel and W.W. Warren Jr. *Fluid Metals*, Princeton Univ. Press.
[17] W.G Hoover, et al. Journal of Chemical Physics **52**, 4931 (1970).

Distribution

1 MS 9018 Central Technical Files, 8945-1
2 MS 0899 Technical Library, 9616
3 MS 0123 LDRD office
4 MS 1186 Thomas Mattsson
4 MS 1186 Michael Desjarlais